

Contents lists available at ScienceDirect

Journal of Catalysis

journal homepage: www.elsevier.com/locate/jcat



Beyond upper bound estimates of active site densities in heterogeneous catalysis: A note on the critical role of titrant pressure



Sadia Afrin, Praveen Bollini*

William A. Brookshire Department of Chemical & Biomolecular Engineering, University of Houston, 4722 Calhoun Rd., Houston, TX 77004, USA

ARTICLE INFO

Article history: Received 3 March 2022 Revised 17 May 2022 Accepted 2 June 2022 Available online 11 June 2022

Keywords: In-situ titrations Cerium oxide Hydrogenation Active site density Turnover frequency

ABSTRACT

In-situ titrations employed in the estimation of active site densities oftentimes only provide upper bound estimates, not true active site densities. Discounting unselective contributions that result in a disparity between the two requires a treatment of transient titration data more nuanced than merely integrating under the titrant breakthrough curve. Three methods for estimating site densities (and turnover frequencies) are presented in the context of ceria-catalyzed ethene hydrogenation, and their strengths and limitations discussed. Readily accessible supra-monolayer coverages of CO prevalent on ceria surfaces help bring into relief considerations relating to unselective adsorption and active site heterogeneity common, yet infrequently addressed, in the characterization of heterogeneous catalysts using in-situ titration methods.

© 2022 Elsevier Inc. All rights reserved.

1. Introduction

In-situ chemical titrations are employed extensively toward determination of active site densities prevalent on heterogeneous catalyst surfaces, and CO a commonly used titrant in this regard. [1–4] Such titrations involve interpretation of reaction rate diminution resulting from introduction of titrant into the feed stream, and in most cases assume adsorption site density to serve as a reliable proxy for active site density. Adsorption site densities, however, in principle only provide upper bounds on active site densities owing to the near-inevitable presence of unselective adsorption -adsorption onto sites that may be similar from a titrant binding standpoint but dissimilar (or absent) from a reactivity standpoint. [5] We posit that the intentional use of titrant pressures low enough as to effect population, exclusively, of active, not adsorption sites, only a fraction of which may participate in catalytic turnovers, can enable estimation of plausible values of active site densities, unlike implausible ones obtained at higher titrant pressures. We note that titrations with nitrogencontaining titrants are typically conducted at significantly lower titrant pressures than those employing CO, [5-9] albeit not necessarily at pressures low enough as to entirely eliminate unselective adsorption, as shown recently by the Kumar et al. [9] Unlike most in-situ titration experiments in which unselective adsorption may in principle be masked by the transient nature of titration data,

supra-monolayer coverages of CO achieved readily over reduced ceria surfaces at temperatures of relevance to ethene hydrogenation catalysis enable the clear demonstration of finite CO adsorptive contributions originating from spectator sites populated at pressures greater than those required to saturate coordinatively unsaturated cerium. We discuss in this context strategies for minimizing contributions from unselective adsorption and active site heterogeneity that may warrant consideration in the characterization of heterogeneous catalysts more generally.

2. Results and discussion

2.1. Ethene hydrogenation site densities: The plausible and the implausible

Bulk ceria reduced at 773 K under 27 kPa H₂ catalyzes ethene hydrogenation at 448 K at areal rates much greater than those exhibited when fully oxidized (Fig. S1, SI), consistent with a prior publication by Minachev et al. [10] that reports increases in areal hydrogenation rates upon reduction under hydrogen at 873–1073 K. Pyridine adsorption onto Lewis acidic cerium cations have been demonstrated previously in the literature; [1,11–12] its introduction at a pressure of 15.5 Pa into the feedstream with ethene and hydrogen at 448 K results in the complete elimination of hydrogenation rates (Fig. S3a, SI). In-situ FTIR spectra of bulk ceria samples exposed to pyridine at 448 K indicate the appearance of bands at 1594 cm⁻¹ and 1440 cm⁻¹ corresponding, respectively, to the 8a and 19b modes of the CCN vibration resulting from

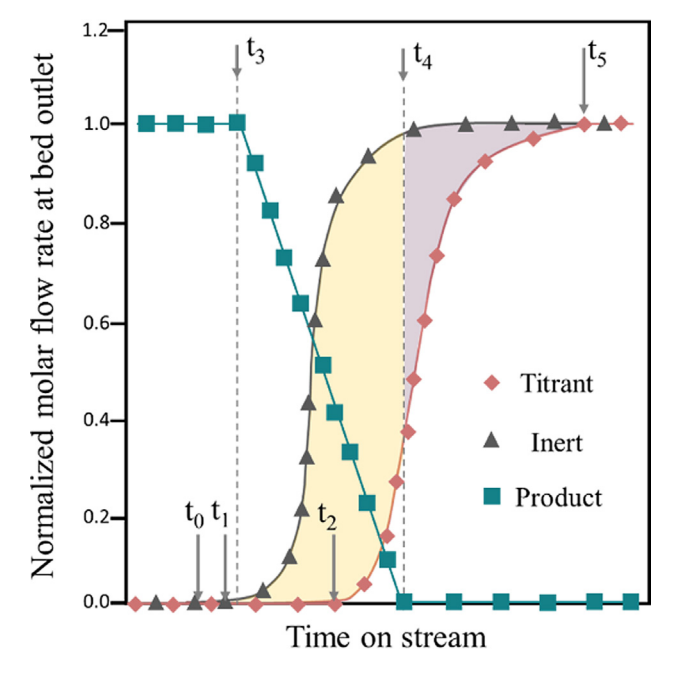
^{*} Corresponding author. E-mail address: ppbollini@uh.edu (P. Bollini).

S. Afrin and P. Bollini Journal of Catalysis 413 (2022) 76–80

pyridine binding onto coordinatively unsaturated cerium sites (Fig. S4, SI). [1,11–13] The absence of characteristic bands expected at 1545 cm⁻¹ for ring vibrations corresponding to pyridine bonded to Brønsted acid sites, or at 2450 cm⁻¹ for N⁺-H vibrations [14] (Fig. S4, inset b, SI), suggest an absence of pyridinium ions on reduced ceria surfaces, consistent with previously reported literature indicating the lack of pyridine binding onto Brønsted acid sites on ceria surfaces at room temperature. [1,11] Only slight perturbations (12% reduction) were observed in the O-H stretching region upon introduction of pyridine (Fig. S5, SI), suggesting that hydrogenative turnovers likely do not occur over hydroxyls, as long as they are all carry an identical catalytic propensity. In-situ FTIR and pyridine titration data therefore suggest that binding onto coordinatively unsaturated cerium tends to be sufficient to eliminate the entirety of measured ethene hydrogenation rates, and that active site counts exceeding the density of surface cerium, although still useful as upper bound estimates, are nevertheless inaccurate representations of the true densities of active sites effectuating hydrogenative turnovers.

2.2. Differentiating adsorption site densities from active site densities

Scheme 1 depicts time scales associated with the various observations ensuing titrant introduction in an in-situ titration experiment. The feed stream in a titration experiment is switched from one containing solely reactants to one also containing titrant at time t0, as a consequence of which product formation rates begin to drop below their steady state value at time t3, which can in many cases lie in the vicinity of t - the time at which the inert tracer breaks through. The concurrence between these two timescales reflects merely the identical nature of hydrodynamic delays for both titrant and inert tracer prior to their contact with the catalyst bed, combined with minimal adsorption of inert onto the catalyst surface. The titrant breaks through the bed at time t2 (Scheme 1),



Scheme 1. Depiction of timescales involved in the transient in-situ titration of active sites on heterogeneous catalyst surfaces. The titrant is introduced into the feedstream at t0, the inert tracer breaks through the catalyst bed at t1, the titrant breaks through the bed at t2. t3 represents the time at which measured product formation rates start to decrease with time-on-stream, t4 the time at which product formation rates are eliminated, and t5 the time at which the bed becomes saturated in titrant at the titrant pressure under consideration.

which can either coincide with or exceed t1 - the breakthrough time for the inert tracer - depending on the degree of dispersion of the titrant concentration front as determined by the mass and heat transfer properties of the system under consideration. Product formation rates fall to their lowest value (zero in this case) at time t4, and the bed becomes saturated in titrant at t5, with t5 necessarily either coinciding with or exceeding t4 owing to the fact that adsorptive processes responsible for titrative effects cease to occur at t5, implying no further reduction in product formation rates can be noted past this point in time. The amount of titrant adsorbed in the bed at equilibrium can be obtained by multiplying the area between the breakthrough curves highlighted in Scheme 1 by the molar flow rate of titrant entering the bed:

$$nT = \dot{n} \times \int_{t_1}^{t_5} (Y_{Tracer} - Y_{Titrant}) dt$$
 (1)

where n_T represents the total moles of titrant adsorbed, \dot{n} the inlet molar flow rate of titrant, and Y_{Tracer} and $Y_{Titrant}$ the normalized molar flow rates of tracer and titrant, respectively.

Transient responses for CO (m/z = 12), Ar (m/z = 40), and ethane (m/z = 30) when co-feeding 0.9 kPa CO with 3.3 kPa ethene and 98 kPa hydrogen indicate a complete elimination of ethane formation rates (Fig. S7b, SI), suggesting that CO, like pyridine, can titrate the entirety of the hydrogenation active site pool on reduced ceria surfaces. The total quantity of CO adsorbed calculated using equation (1) exceed monolayer coverages (Fig. 1), and hence serve as unreliable proxies for active site densities that are necessarily capped at 1 mol sites per mol surface Ce; these adsorption site densities, although of general utility in deciphering upper bounds for active site densities, fail to provide meaningful insights in the context of the reaction system under consideration. CO adsorption site densities calculated using equation (1) - the method most commonly used in the literature to estimate active site densities, [2,15–17] not only exceed monolayer coverages, but also increase monotonically with CO pressure (Fig. 1), consistent with their interpretation as adsorption site densities, not active site densities, with the latter, unlike the former, expected to be independent of CO pressure. Similar increases in site density with pyridine pressure have been noted Kumar et al. during the titration of Brønsted

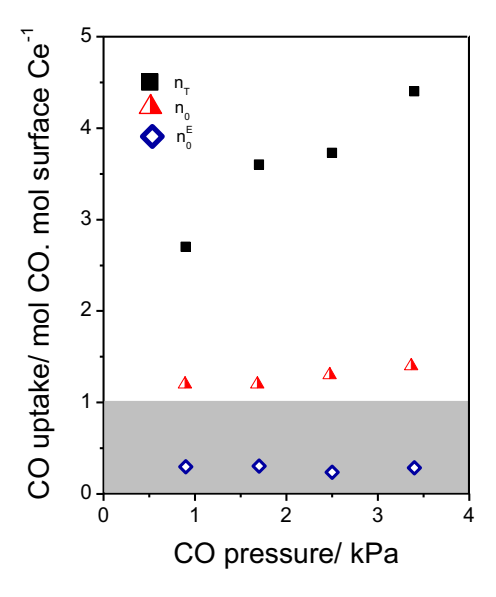


Fig. 1. CO adsorption uptakes calculated using equations (1) (n_T) , 2 (n_0) and linear extrapolation (Fig. S12, SI) of in-situ titration data (n_0^E) . The shaded area represents the plausible range of values for active site density. Reaction conditions: 0.9–3.4 kPa CO, 0.9–3.4 kPa Ar, 3.3 kPa ethene, 98 kPa H₂, and balance He with a total flow rate of 2.4 cm³ s⁻¹ at 448 K.

S. Afrin and P. Bollini Journal of Catalysis 413 (2022) 76–80

acid sites in phosphorus-modified zeosils; [9] estimated acid site densities in their study, although accurately analyzed, remain lower than Brønsted acid site counts for the unmodified zeolite. Site densities presented thus far in our study, on the other hand, are *necessarily* incorrect owing to the fact that they significantly exceed surface cerium densities, and therefore point to a clear example of disparities between adsorption and active site densities – disparities that may otherwise be challenging to evidence definitively. Although lower CO pressures provide more meaningful upper bound estimates for active site densities, measuring adsorption site densities that lie within a plausible range of values for active site density require CO pressures lower than those that can in the current case be used to generate reproducible titration data ($\ll 0.5 \text{ kPa}$).

The overestimation of active site densities due to unselective adsorption is rather common when using in-situ titration protocols, with the fraction of sites titrated that contribute to measured reaction rates being challenging to deconvolute - a fact noted previously in the context of hydrogenation reactions over metal sulfide hydrotreating catalysts by the Lercher group. [15] Unlike previous examples in which definitive methods for discounting unselective adsorption may not be immediately obvious, adsorption of the titrant CO in the current case is noted to continue past the time (t4) at which ethane formation rates become negligible (Scheme 1 and Fig. S7, SI). The catalyst bed continues to adsorb CO past t4 as a consequence of adsorption events that are necessarily unrelated to catalytic turnovers and hence cannot involve active sites, the entirety of which are titrated prior to t4. Contributions from adsorption occurring subsequent to the cessation of titrative events that reduce product formation rates can be eliminated from estimated active site densities by integrating upto t4, not t5, using the following equation:

$$n0 \ = \ \dot{n} \times \int_{t_1}^{t_4} (Y_{\textit{Tracer}} - Y_{\textit{Titrant}}) dt \eqno(2)$$

where n_0 represents the total calculated number of active sites in the bed. Active site densities estimated (using equation (2)) by discounting adsorptive contributions past the point of elimination of product formation rates (Fig. 1) yield site densities that are a) relatively independent of CO pressure, unlike adsorption site densities (n_T) that increase monotonically with CO pressure and b) approximate, within error, the density of surface cerium, i.e. the maximum number of active sites that can be accommodated on the surface, as inferred from pyridine titration data. Titration features noted in this study therefore allow us to capture and eliminate from consideration contributions from titrant adsorption that are verifiably unselective owing to their irrelevance to rate reduction; the unselective nature of such contributions can oftentimes be masked by the hydrodynamics of titrant front propagation through the catalyst bed. Although eliminating a fraction of the unselective contributions to CO adsorption, restricting integration upto t4 does not necessarily eliminate all unselective contributions to adsorption, nor does it evaluate in any way the uniformity of a catalytic surface (or lack thereof). Further evaluating these considerations requires recasting transient in-situ titration data presented thus far in terms of moles of CO adsorbed per mole surface cerium, i.e. the titrant loading, rather than time on-stream.

2.3. Do all surface cerium sites contribute equally to ethene hydrogenation?

The CO loading at any time-on-stream value can be calculated by integrating the difference between molar flow rates of CO and the titrant using the following equation:

$$n_{s} = \dot{n} \times \int_{t_{1}}^{t} (Y_{Tracer} - Y_{Titrant}) dt$$
 (3)

where the integration is carried out upto any time-on-stream value of interest. Recasting product formation rates as a function of CO loading reveals non-linear effects of CO adsorption on ethene hydrogenation (Fig. 2). Ethene hydrogenation rates are more sensitive to CO adsorption at low CO loadings than at high loadings, indicating either a) unselective adsorptive contributions prior to rate elimination the contributions of which increase with timeon-stream/CO loading or b) heterogeneity in active site speciation. with sites titrated at lower CO pressures being disproportionately active compared to those titrated at higher pressures. Definitive differentiation between these two scenarios requires quantitative analysis of equilibrium and dynamic CO adsorption behavior at 448 K - analyses that remain outside the scope of this research note. Nevertheless, we surmise that differences in the propensity of active sites toward ethene hydrogenation are the more likely explanation for the observed non-linearity in titration data due in part to the partial (not complete) rate recovery upon elimination of CO from the feed stream (Fig. S3, SI), suggesting participation, at the very least, of two distinct ethene hydrogenation sites that each differ in the extent of reversibility of CO binding at 448 K. Sites titrated earlier in time/CO loading are likely more active, and encounter (on average) lower CO pressures, and hence exhibit significantly greater sensitivity of measured rates to CO loading (Fig. 2). Sites that are less active toward ethene hydrogenation, in contrast, are populated later in the titration experiment, and therefore result in a lower sensitivity of rates to CO loading at later times. An additional observation in favor of invoking site heterogeneity rather than unselective adsorption in accounting for the non-linearity in titration data relates to the fact that rates appear to track similarly with CO loading regardless of inlet CO pressure in a range where the former are clearly strongly dependent on the latter. Finite CO loadings are achieved during the titration pro-

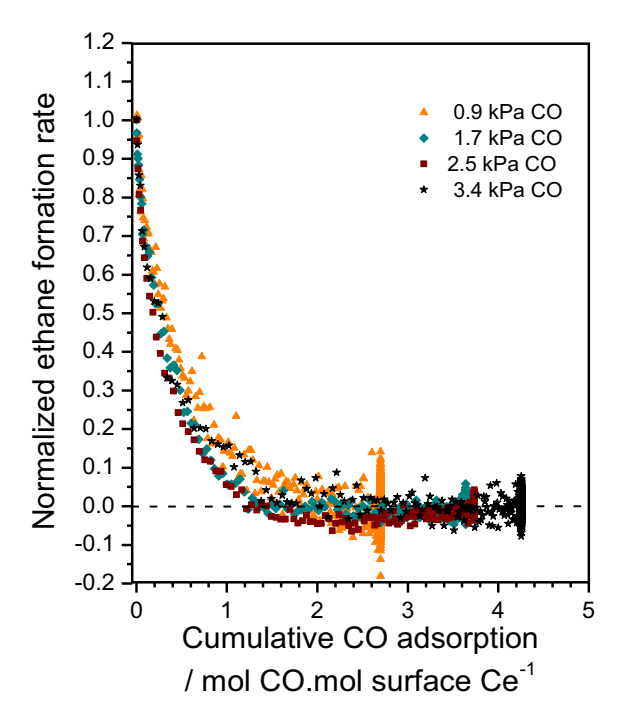


Fig. 2. Titration of ethene hydrogenation active sites over reduced ceria surfaces at different CO partial pressures. Ethane formation rates are normalized by their average value at steady state prior to titration, and CO loadings were calculated using eq'n 3. Reaction conditions: 448 K, 0.9–3.4 kPa CO, 0.9–3.4 kPa Ar, 3.3 kPa ethene, 98 kPa $\rm H_{2}$, balance He, total flow rate: 2.4 cm³ s⁻¹.

S. Afrin and P. Bollini Journal of Catalysis 413 (2022) 76–80

cess through the progression of a concentration front that changes in magnitude with varying inlet CO pressure (Scheme S1, SI), implying that identical CO loadings on the catalyst surface should result in larger rate reductions at lower CO pressures rather than at higher CO pressures because these higher gas phase CO pressures in the 'CO-loaded' portion of the bed cause greater unselective contributions to a given CO loading. In other words, identical CO loadings, when accessed through multiple CO pressures, should owe their provenance to unequal distributions of selective versus unselective sites, with the preponderance of the latter increasing with inlet CO pressure and therefore resulting in lower sensitivities of rates with total CO loading. The collapsing of rate data for the four titrant pressures that demonstrably lie in a range where unselective adsorption does indeed occur (Fig. 2), combined with the invariance in active site densities obtained when integrating the titrant breakthrough curve upto the point of rate elimination (Fig. 1) suggest that non-linear titration curves could potentially result from heterogeneity in active site propensity toward hydrogenative turnovers, and not merely as a consequence of unselective adsorption occuring at sub-monolayer coverages.

Assuming the initial linear rate of decrease in ethane formation rates with CO loading to be resulting predominantly from titration of the most active sites, the abscissa obtained upon extrapolation of this linear rate reduction can be inferred as providing the density of the most active sites on the reduced ceria surface - a treatment equivalent to assuming initial rates of rate decrease in Fig. 2 to be reflective of the turnover frequencies (TOFs) corresponding to these sites that are more active than the rest. Site densities obtained using this extrapolation method appear insensitive to CO pressure used (0.24-0.30 mol/mol Ce_s, Fig. 1), consistent with initial rate reduction profiles reflecting the titration of solely one type of active site regardless of CO pressure used. Regardless of the precise basis for the observed non-linearity in titration data unselective adsorption or active site heterogeneity - such rate extrapolations applied after recasting titration data as a function of titrant loading carry specific, interpretable bases, unlike extrapolations in the time domain [18–19] that (in our opinion) rarely do.

TOF values can now be calculated using any of the three sets of assumptions used to estimate site densities - total CO adsorption capacities (n_T), adsorption capacities corresponding to hydrogenation rate elimination (n_0) , and site densities obtained by extrapolating the initial linear rate of decrease in rates as a function of CO loading as shown in Fig. S12 of the Supporting Information (n_0^E) . As expected, TOF values trend inversely with site densities shown in Fig. 1, and appear to be invariant in CO pressure regardless of the method used to estimate site densities (Fig. 3). In fact. TOFs vary only minimally (0.232 ± 0.048 ks⁻¹) even when using as site density proxies total adsorption capacity values (n_T) that clearly overestimate active site densities by including adsorption onto sites extraneous to those that effect ethene hydrogenation, suggesting that an invariance in TOF values with titration conditions can serve as insufficient justification for the validity of reported site counts. More specifically, the measurement of 'similar' TOF values when changing titrant pressure in regions of the titrant adsorption isotherm sufficiently close to saturation where titrant pressure has little to no effect on surface coverage [2,15] may constitute rigorous proof of neither the validity nor the utility of reported site counts. It may in fact be argued that the utility of measured site counts are predicated on maintaining sufficient distance from saturation and a concomitant meaningful degree of proximity to the Henry's law regime such that a finite sensitivity of titrant loading to titrant pressure can be exploited toward validating reported site densities. Although pressure ranges low enough where every titrant adsorption event corresponds to the elimination of an active site ($\ll 0.5$ kPa) remain elusive for the sys-

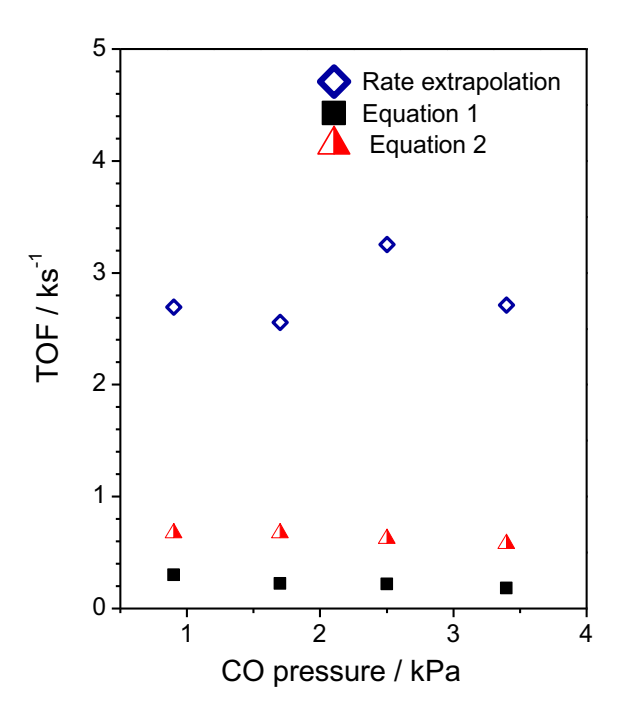


Fig. 3. Ethene hydrogenation turnover frequencies (TOFs) based on site counts estimated using three different methods. Site counts used in the estimation of TOFs are shown in Fig. 1.

tem under consideration, the results do in fact appear to disprove site counts estimated using commonly employed methods for treating in-situ titration data, and are valuable in that they demonstrate, clearly, the critical role of titrant pressure in assessing whether adsorption capacities otherwise reported as active site densities serve merely as upper bounds, or carry potential chemical significance as accurate proxies for active site densities.

3. Conclusions

Reduced ceria surfaces catalyze ethene hydrogenation, the rates of which at 448 K can be titrated entirely through pyridine binding onto coordinatively unsaturated surface cerium and (alternatively) through CO binding at supra-monolayer coverages at titrant pressures as low as 3.4 kPa. Adsorptive contributions of CO, when calculated upto the point of elimination of hydrogenation rates, yield plausible active site densities, unlike total adsorption capacity values used more commonly in the literature that yield implausible values significantly exceeding the density of surface cerium. Nonlinearity of titration curves in the CO loading domain can be interpreted as originating either from unselective adsorption or active site heterogeneity, either of which could potentially be accounted for by extrapolating the initial sensitivity of rates to titrant loading. More generally, titrant pressure appears to be a key experimental design variable carrying perceptible implications on the rigorous application of chemical titration data to yield active site densities the accuracy of which are influenced heavily by the distance of titrant pressure values employed from those required for active site saturation.

Declaration of Competing Interest

The authors declare that they have no known competing financial interests or personal relationships that could have appeared to influence the work reported in this paper.

Acknowledgements

S. Afrin and P. Bollini

The authors acknowledge support from the National Science Foundation (Award # 1916133).

Appendix A. Supplementary material

Supplementary data to this article can be found online at https://doi.org/10.1016/j.jcat.2022.06.006.

References

- [1] C. Binet, M. Daturi, J.C. Lavalley, IR study of polycrystalline ceria properties in oxidised and reduced states, Catal. Today 50 (2) (1999) 207–225.
- [2] W.S. Lee, A. Kumar, Z. Wang, A. Bhan, Chemical titration and transient kinetic studies of site requirements in Mo₂C-catalyzed vapor phase anisole hydrodeoxygenation, ACS Catal. 5 (7) (2015) 4104–4114.
- [3] W. An, A.E. Baber, F. Xu, M. Soldemo, J. Weissenrieder, D. Stacchiola, P. Liu, Mechanistic study of Co titration on CuxO/Cu(111) (X≤2) surfaces, ChemCatChem 6 (8) (2014) 2364–2372.
- [4] A. Yee, S.J. Morrison, H. Idriss, A study of the reactions of ethanol on CeO₂ and Pd/CeO₂ by steady state reactions, temperature programmed desorption, and in situ FT-IR, J. Catal. 186 (2) (1999) 279–295.
- [5] C.D. Baertsch, K.T. Komala, Y.H. Chua, E. Iglesia, Genesis of Brønsted acid sites during dehydration of 2-butanol on tungsten oxide catalysts, J. Catal. 205 (1) (2002) 44–57.
- [6] J.S. Bates, B.C. Bukowski, J.W. Harris, J. Greeley, R. Gounder, Distinct catalytic reactivity of Sn substituted in framework locations and at defect grain boundaries in Sn-zeolites, ACS Catal. 9 (7) (2019) 6146–6168.
- [7] J.S. Bates, B.C. Bukowski, J. Greeley, R. Gounder, Structure and solvation of confined water and water-ethanol clusters within microporous Brønsted acids and their effects on ethanol dehydration catalysis, Chem. Sci. 11 (27) (2020) 7102–7122.

- [8] J.F. DeWilde, H. Chiang, D.A. Hickman, C.R. Ho, A. Bhan, Kinetics and mechanism of ethanol dehydration on γ-Al₂O₃: the critical role of dimer inhibition, ACS Catal. 3 (4) (2013) 798–807.
- [9] G. Kumar, L. Ren, Y. Pang, X. Li, H. Chen, J. Gulbinski, P.J. Dauenhauer, M. Tsapatsis, O.A. Abdelrahman, Acid sites of phosphorus-modified zeosils, ACS Catal. 11 (15) (2021) 9933–9948.
- [10] K.M. Minachev, Y.S. Khodakov, V.S. Nakhshunov, Activity and mechanism of the catalytic action of rare-earth oxides in low-temperature ethylene hydrogenation, J. Catal. 49 (2) (1977) 207–215.
- [11] M.I. Zaki, G.A.M. Hussein, S.A.A. Mansour, H.A. El-Ammawy, Adsorption and surface reactions of pyridine on pure and doped ceria catalysts as studied by infrared spectroscopy, J. Mol. Catal. 51 (2) (1989) 209–220.
- [12] M.E.Z. Velthoen, S. Nab, B.M. Weckhuysen, Probing acid sites in solid catalysts with pyridine UV-vis spectroscopy, Phys. Chem. Chem. Phys. 20 (33) (2018) 21647–21659.
- [13] Z. Wu, A.K.P. Mann, M. Li, S.H. Overbury, Spectroscopic investigation of surface dependent acid base property of ceria nanoshapes, J. Phys. Chem. C 119 (13) (2015) 7340–7350.
- [14] M.I. Zaki, M.A. Hasan, F.A. Al-Sagheer, L. Pasupulety, In situ FTIR spectra of pyridine adsorbed on SiO₂–Al₂O₃, TiO₂, ZrO₂ and CeO₂: general considerations for the identification of acid sites on surfaces of finely divided metal oxides, Colloids Surfaces A 190 (2001) 261–274.
- [15] F. Vogelgsang, H. Shi, J.A. Lercher, Toward quantification of active sites and site-specific activity for polyaromatics hydrogenation on transition metal sulfides, J. Catal. 403 (2021) 98–110.
- [16] B. Yeh, S.P. Vicchio, S. Chheda, J. Zheng, J. Schmid, L. Löbbert, R. Bermejo-Deval, O.Y. Gutiérrez, J.A. Lercher, C.C. Lu, et al., Site densities, rates, and mechanism of stable Ni/UiO-66 ethylene oligomerization catalysts, J. Am. Chem. Soc. 143 (48) (2021) 20274–20280.
- [17] P. Deshlahra, R.T. Carr, S.H. Chai, E. Iglesia, Mechanistic details and reactivity descriptors in oxidation and acid catalysis of methanol, ACS Catal. 5 (2) (2015) 666–682
- [18] J.F. DeWilde, C.J. Czopinski, A. Bhan, Ethanol dehydration and dehydrogenation on γ -Al₂O₃: mechanism of acetaldehyde formation, ACS Catal. 4 (12) (2014)
- [19] M.M. Sullivan, A. Bhan, Acid site densities and reactivity of oxygen-modified transition metal carbide catalysts, J. Catal. 344 (2016) 53–58.